Asociación Argentina
de Mecánica Computacional

Mecánica Computacional Vol XXIX, págs. 3291-3303 (artículo completo)
Eduardo Dvorkin, Marcela Goldschmit, Mario Storti (Eds.)
Buenos Aires, Argentina, 15-18 Noviembre 2010

EXPERIMENTAL AND NUMERICAL STUDY OF THE AERODYNAMIC BEHAVIOUR OF A SIMPLIFIED ROAD VEHICLE

Hugo G. Castro[a,b], Rodrigo R. Paz[a], Mario A. Storti[a], Victorio E. Sonzogni[a], Jorge O. Marighetti[b] and Mario E. De Bortoli[b]

[a]*Centro Internacional de Métodos Computacionales en Ingeniería (CIMEC), INTEC-CONICET-UNL, Guemes 3450, (S300GLN) Santa Fe, Argentina, http://www.cimec.org.ar*

[b]*Grupo de Investigación en Mecánica de Fluidos, Universidad Tecnológica Nacional, Facultad Regional Resistencia, French 414, Chaco, Argentina, hugoguillermo_castro@yahoo.com.ar*

Keywords: Vehicle aerodynamics, PETSc-FEM, Parallel computing, Wind tunnel.

Abstract. Understanding ground vehicles aerodynamics allows us to optimize the operation of a wide spectrum of road vehicles, that ranges from road passenger transport (cars, buses, trains) to road comercial transport (trucks and trains). Within the first group, the so called "double-deck buses" have awakened an increasing interest, given their extensive utilization in our country. According to this, a series of investigations were initiated at the CIMEC (Centro Internacional de Métodos Computacionales en Ingeniería) focussing in the modeling and the understanding of the aerodynamic characteristics of these large vehicles.

As part of an early stage of these investigations, we present in this paper both, numerical and experimental simulation of wind flow passing through vehicles. A simplified model, knowing as Ahmed body was studied and the drag of the model and pressure coefficients on the model rear end were compared between both techniques.

Coupling the wind field with the vehicle dynamics will be the next step in the investigations so a discussion about how to implement Fluid-Structure Interaction (FSI) to this specific problem is also provided.

The numerical model was implemented using PETSc-FEM, which is an open source CFD (Computational Fluid Dynamics) tool based in the Finite Element Method (FEM) using distributed processing and object oriented programming, developed at the CIMEC (http://www.cimec.org.ar/petscfem). The experimental tests were developed in the "Jacek Gorecki" boundary layer wind tunnel, located in the Facultad de Ingeniería de la Universidad Nacional del Nordeste (UNNE) sited in Resistencia, Chaco, Argentina.

1 INTRODUCTION

Understanding ground vehicles aerodynamics allows us to optimize the operation of a wide spectrum of road vehicles, that ranges from road passenger transport (cars, buses, trains) to road comercial transport (trucks and trains). Within the first group, the so called "double-deck buses" have awakened an increasing interest, given their extensive utilization in our country. According to this, a series of investigations were initiated at the CIMEC focussing in the modeling and the understanding of the aerodynamic characteristics of these large vehicles.

From its origins to the present, Computational Fluid Dynamics (CFD) allowed us to improve understanding of the physical phenomena arising from flows over bluff boddies. As ground vehicles have geometries that can be assimilated into this category, several numerical procedures used on flows over bluff boddies have been applied to vehicle aerodynamics study. Reynolds averaged Navier-Stokes (RANS) approach was widely used in past investigations of vehicle aerodynamics (Basara et al., 2001; Guilmineau, 2008) in some cases due to computational resources limitations and later with the improvement of computational power and efficiency, large eddie simulations (LES) has become an attactive methodology, (Krajnovic, 2002; Hinterberger et al., 2004; Krajnovic and Davison, 2004a; Franck et al., 2003, 2004).

As real vehicles have complex geometries, a simplified (generic) vehicle called Ahmed body was proposed as a reference model for experimental and computational tests, (Ahmed et al., 1984). Thus, with this model as a standard benchmark, general geometric properties can be analized and their effects on the flow can be studied.

Several investigations has been evoked to implement both, numerical and experimental studies of the flow around this particular model. According to Guilmineau (2008), RANS simulations doesn't fits well the flow around the Ahmed body for a slant angle of 25° while for an angle of 30° this approach works well. This implies that RANS simulations depends strongly on the implemented turbulence model and geometric characteristics of the problem. Meanwhile, using LES on this particular problem had demostrated that it can predict the location at which the flow separates from the model skin and the flow structure on the wake, (Krajnovic and Davison, 2004b).

While high performance computing are widely use to assist in the solution of vehicle aerodynamics problems, the wind tunnel is still the major and most reliable development tool, (Cooper, 1993). However, the accuracy of the simulation depends on how well and how much of the prototype environment is simulated in the wind tunnel.

As part of an early stage of these investigations, we present in this paper both, numerical and experimental simulation of wind flow passing through vehicles. A simplified model, knowing as Ahmed body was studied and drag force of the model and pressure coefficients on the model rear end were compared between both techniques.

2 SIMPLIFIED ROAD VEHICLE MODEL: AHMED BODY

The aerodynamic characteristics of road vehicles have many features that are similar to those present in civil-engineering structures, i.e. are dominated by flow separation and are influenced by the atmospheric wind. To study some flow features whithout complex geometries a simplified model is required.

The Ahmed body was first defined and its characteristics described in the experimental work of Ahmed et al. (1984). With a simple geometry, consisting of three parts; a fore body, a mid section and a rear end, see figure (1), the flow around it still retains some characteristics of the flow around real road vehicles. For a more detailed description of the model see the papers of

Franck et al. (2003, 2004).

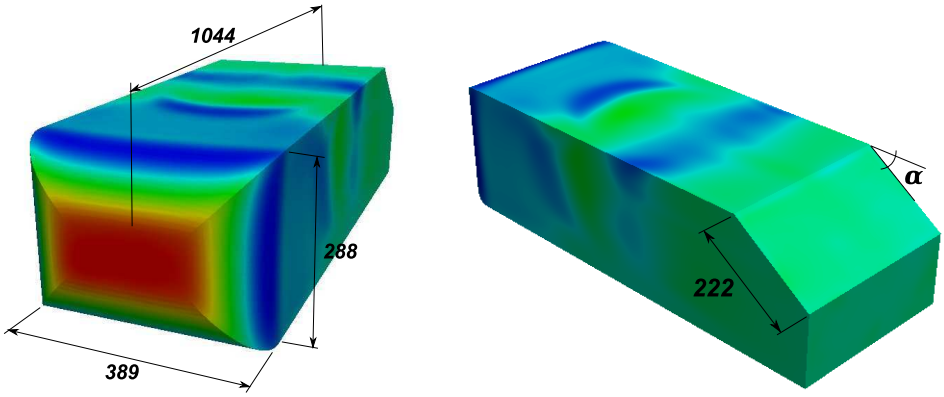

Figure 1: Main dimensions of the simpified model proposed by Ahmed et al. (1984) along with the pressure distribution on its surface.

In the test performed by Ahmed et al. (1984), the model was fixed on cylindrical stilts 50 mm above a ground board 3 m wide and 5 m long, in an open tunnel test section. A wind speed of 60 m/s was used, corresponding to a model length based Reynolds number of 4.29×10^6 and a turbulence intensity less than 0.5%.

The authors found that the major contribution to the pressure drag comes from the slant and vertical base surface of rear end.

3 COMPUTATIONAL SIMULATION

3.1 Numerical method

An incompressible newtonian viscous fluid model is adopted with a bulk velocity of 23.5 m/s, kinematic viscosity $\nu = 1.45 \times 10^{-6}$ m^2/s and density $\rho = 1.225$ kg/m^3. Non-slip boundary condition is prescribed at ground, roof and walls of the domain as well as at the body surface while for the domain outlet, pressure is set to zero.

The simulations were performed with the PETSs-FEM code developed at the CIMEC (http://www.cimec.org.ar/petscfem). PETSc-FEM is a general purpose, parallel, multi-physics finite element program which has been used in many applications including analysis of petroleum refinery processes, aerospace industry, environmental impact assessment and siderurgical processes.

The Finite Element Method is used to solve the momentum and continuity equations for the velocity and pressure at each node and at each time step. SUPG/PSPG discretization scheme of the incompressible Navier-Stokes equations are implemented.

The problem was solved using the *"Aquiles"* cluster which is a beowulf kind of cluster, with 80 nodes Pentium 4 CPU 3.00 GHz and a server Xeon E5335 2.00 GHz, interconnected via a Gigabit Ethernet network.

3.2 Computational domain and inlet boundary conditions

As the aim of this work is to reproduce computationally the wind tunnel flow over road vehicles, the computational domain was adjusted to the main dimensions of the wind tunnel test section. In trying to reproduced it, no advantage was taken of the symmetry of the problem in order to perceive any asymmetry of the solutions. The domain starts at two body lengths in

front and three body lengths behind the model. The width is 2.40 m with 1.80 m height and 6.264 m long, see figure (2). The center of the coordinate system was placed at the inlet plane ($x = 0$ is the symmetry plane, $y = 0$ is the inlet plane, $z = 0$ is the ground plane).

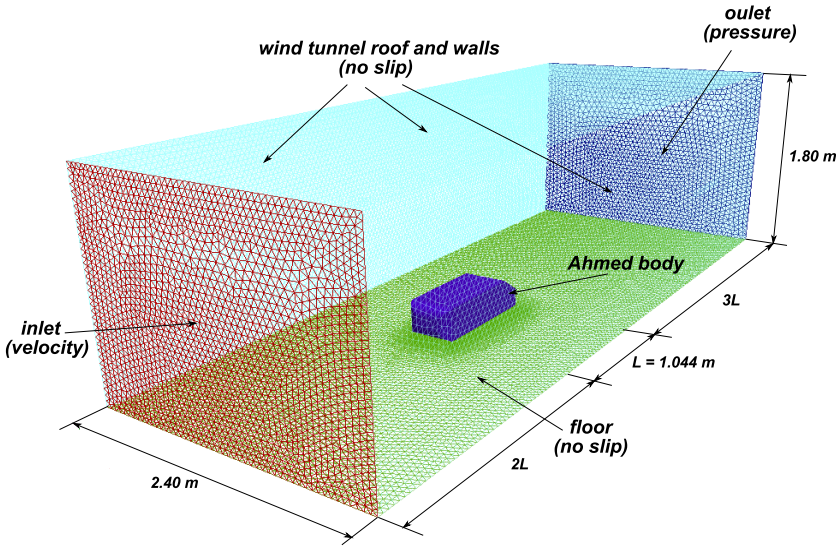

Figure 2: Computational domain geometry and boundary conditions applied to the problem.

Two different configurations of the Ahmed body were studied, with stilts and without stilts. The finite element mesh with stilts consisted in 1716517 tetrahedral elements and 137888 wedge elements, given a number of 1854405 total elements and 379576 nodes. Without stilts, the mesh was composed by 2398332 tetrahedral elements and 115848 wedge elements, given a number of 2514178 total elements and 482420 nodes.

The boundary condition at the inlet of the domain calls for a fully developed flow with boundary layers on roof, walls and floor, as this is the case in the wind tunnel test section. To achieve this condition, mean velocity profiles and turbulence intensity values were adopted in agreement with the values reported by Wittwer and Möller (2000).

Another very important issue to ensure obtaining accurate LES results is to generate a random flow field as an inflow boundary condition (inflow turbulence) satisfying prescribed spatial correlations and turbulence characteristics. There are several methods to achieve this condition namely the *synthesized turbulence* methods: Fourier techniques, POD and digital filter methods; and those belonging to the *precursor simulation* methods, (Tabor and Baba-Ahmadi, 2010). In this work, a method of the former cathegory, proposed by Davison (2007a,b) was implemented. This method states that a turbulent velocity field can be simulated using random Fourier modes:

$$\boldsymbol{u}_t(\boldsymbol{x}) = 2\sum_{n=1}^{N} \hat{u}_n \cos(\boldsymbol{k}_n \cdot \boldsymbol{x} + \psi_n)\boldsymbol{\sigma}_n \tag{1}$$

where $\hat{u}_n$, ψ_n and $\boldsymbol{\sigma}_n$ are the amplitude, phase and direction of Fourier mode n. The direction $\boldsymbol{\sigma}_n$ has $|\boldsymbol{\sigma}_n| = 1$ and the orientation of the vector $\boldsymbol{k}_n$ is chosen randomly on a sphere with radius k_n in order to ensure isotropy of the generated velocity field. The highest wave number is defined based on mesh resolution $\kappa_{max} = 2\pi/(2\Delta)$. The smallest wave number is defined form $\kappa_1 = \kappa_e/2$, where κ_e corresponds to the energy-carrying eddies.

A model spectrum (von-Kármán-Pao spectrum) is used to simulate the shape of the energy spectrum for isotropic turbulence:

$$E(\kappa) = \alpha \frac{u_{rms}}{\kappa_e} \frac{(\kappa/\kappa_e)^4}{[1+(\kappa/\kappa_e)^2]^{17/6}} \exp[-2(\kappa/\kappa_\eta)^2] \tag{2}$$

where κ is the wave number, $\kappa_\eta = \epsilon^{1/4}\nu^{-3/4}$ is the Kolmogorov wave number, ν is the molecular viscosity and ϵ is the turbulence dissipation ratio. u_{rms} is the *rms* value of the velocity fluctuations corresponding to the turbulent kinetic energy, $u_{rms} = 2\overline{k}/3$. There are two "free" paremeters in equation (2); α, which determines the kinetic energy of the spectrum and the wave number κ_e corresponding to the peak of the spectrum.

The require data necessary to implement this synthesized turbulence method can be provided by means a RANS simulation or experimental tests, being the later the approach used in this case.

Once a fluctuating velocity field is generated each time as described above, to create correlation in time the following equation is introduced:

$$\boldsymbol{v}^m(\boldsymbol{x}) = a\boldsymbol{v}^{m-1}(\boldsymbol{x}) + b[\boldsymbol{u}^m(\boldsymbol{x}) + \boldsymbol{u}^{m-1}(\boldsymbol{x})] \tag{3}$$

where m denotes the time step number, $a = \exp(-\Delta t/\tau)$ and $b = \sqrt{(1-a)/2}$, τ being the time scale. Generated inlet velocity fluctuations are shown in figure (3).

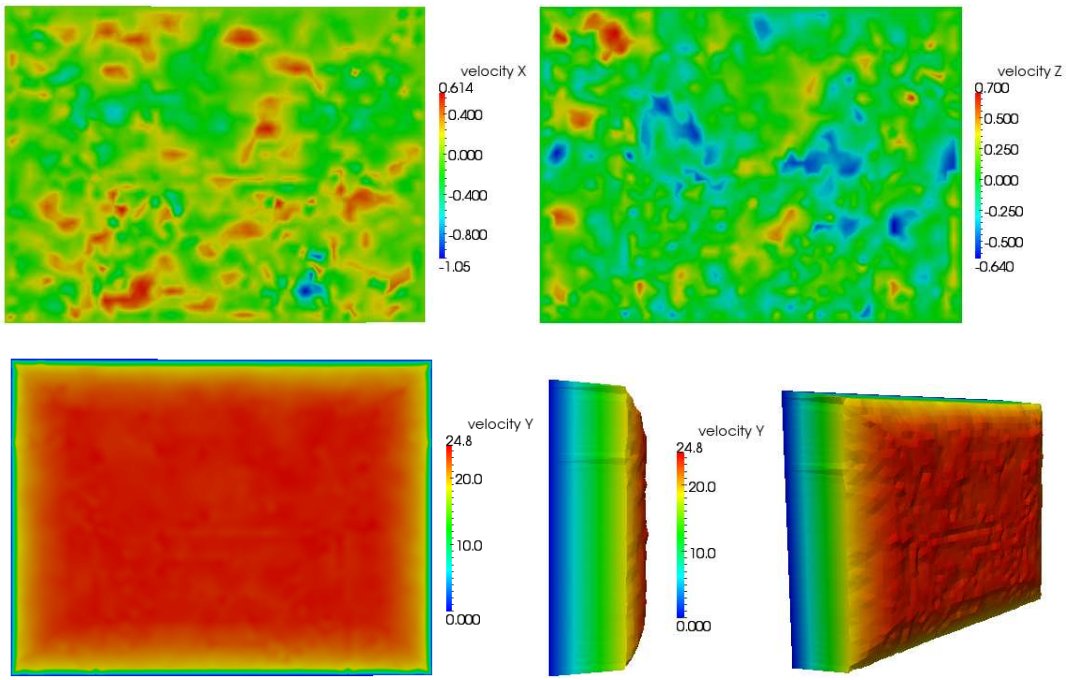

Figure 3: Inlet conditions generated by the synthesized turbulence method.

3.3 Numerical results

The aerodynamic drag and lift forces are computed during the simulation, obtained by adding the viscous and pressure forces around the full three-dimensional geometry at each iteration. Figure (4) shows the time-varying drag coefficient of the Ahmed model without stilts. Mean drag coefficient value was $Cd_{mean} = 0.28$ and *rms* value $Cd_{rms} = 0.014$. In figure (5) it can

be seen the time-varying drag coefficient of the model with stilts, with $Cd_{mean} = 0.357$ and $Cd_{rms} = 0.017$ in this case.

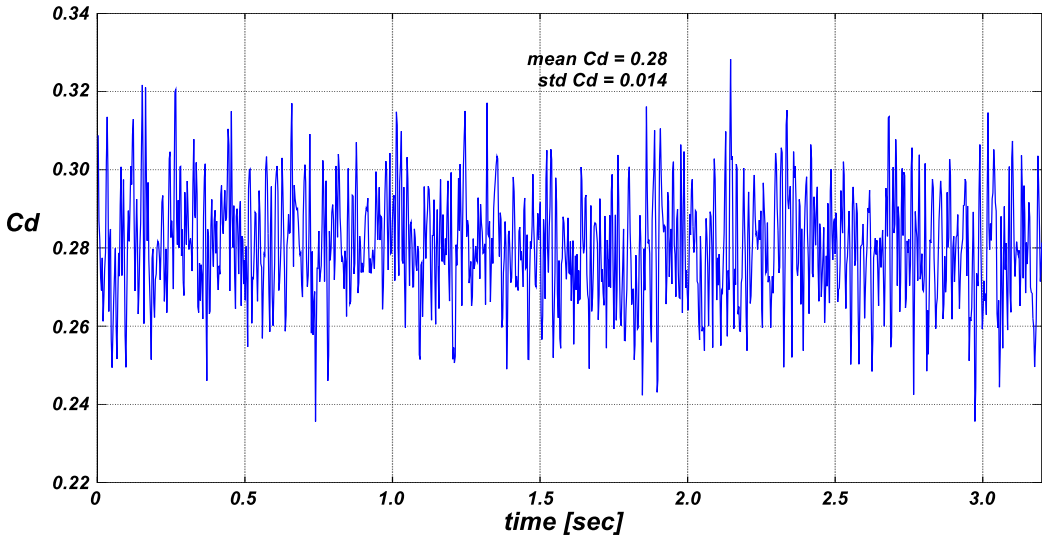

Figure 4: Drag coefficient history of the model without stilts.

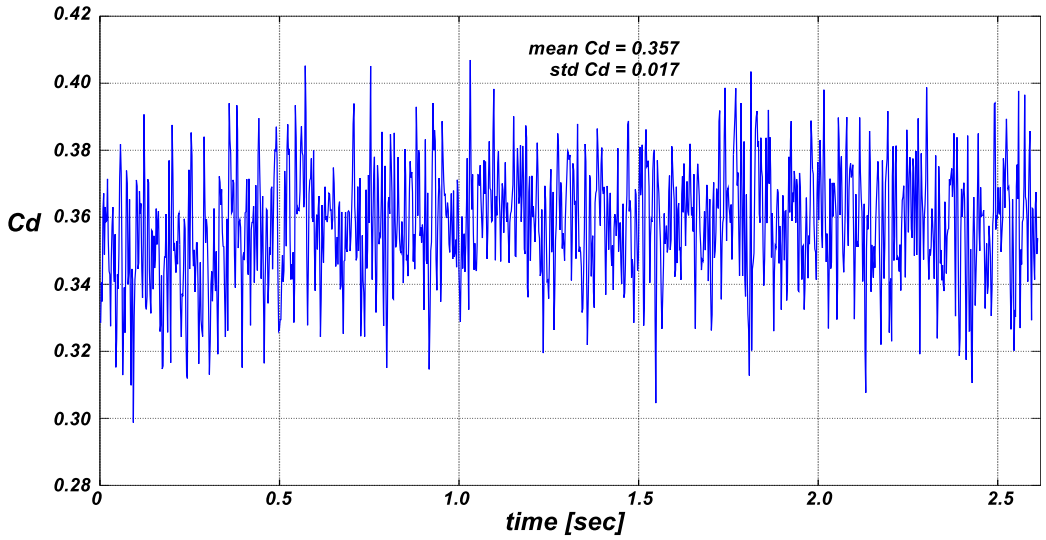

Figure 5: Drag coefficient history of the model with stilts.

Time averaged pressure coeficient distribution is shown in figure (6) corresponding to the rear slanted and vertical planes. The pressure coeficientes C_p were computed using the equation:

$$C_p = \frac{p - p_\infty}{\frac{1}{2}\rho U_\infty^2} \tag{4}$$

where U_∞ is the wind speed, p is the static pressure and p_∞ is the free stream pressure (reference pressure). In this simulations the point of the domain chosen for the pressure and velocity reference was the same (or approximately) as the used in the experimental tests (Pitot-Prandtl tube position).

Monitoring this values until detect some symmetry of the flow around the symmetry plane $(x = 0)$ was used as a criteria for define the averaging time.

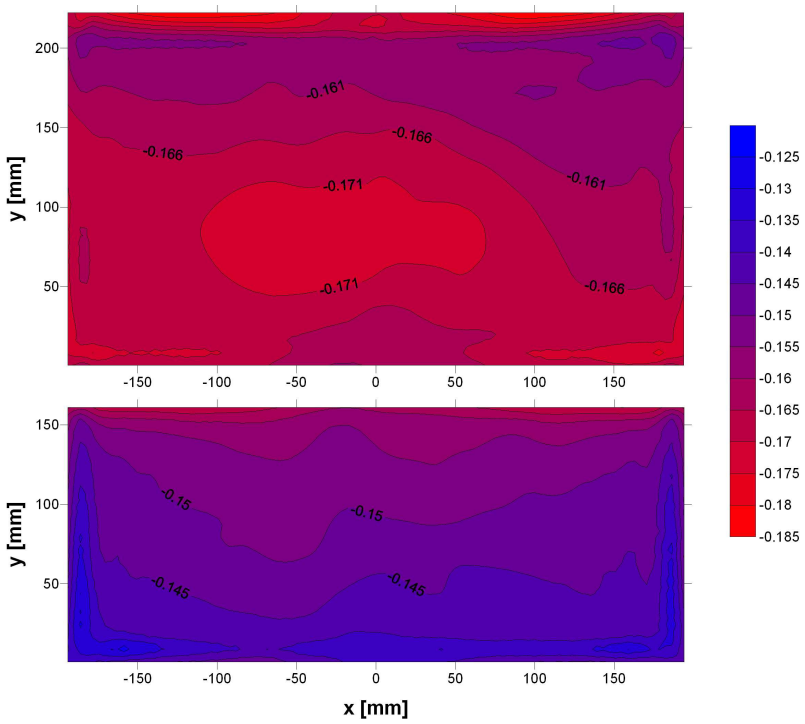

Figure 6: Pressure coefficients distribution over the rear slanted (*up*) and rear vertical (*down*) planes of the model.

The time-averaging solution of the problem is shown in figure (7). Can be seen the presence of two flow separation points. The flow first detaches from the roof surface of the model near the fore body. It then re-attaches onto the same surface to dettached later on the leading edge of the slant. Although the model is quite bluff, the drag characteristics are affected by changes in Reynolds number as the round front part doesn't determine a fix point of separation.

Same observations can be done about figure (8). Delaying the location of the separation point would cause positive pressures regions with a consequent increase in the drag force.

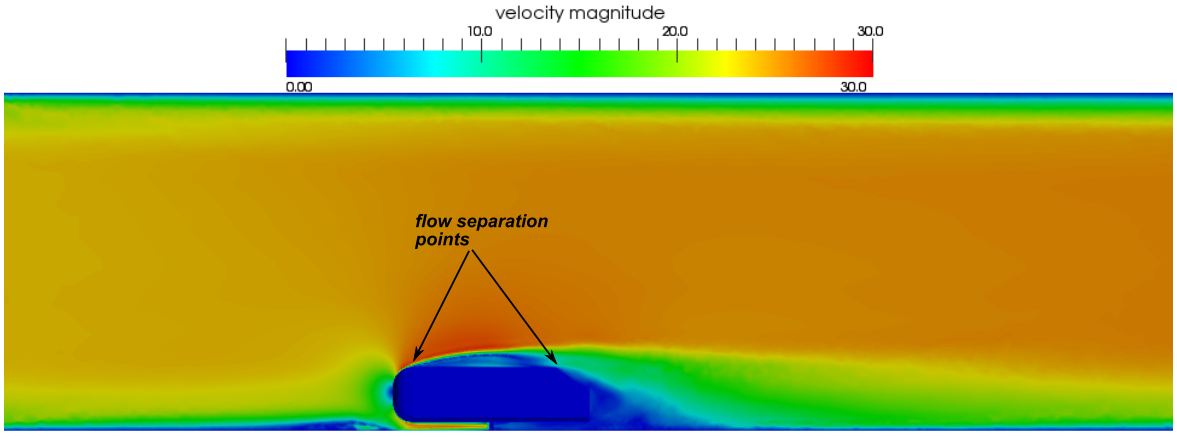

Figure 7: Velocity field obtained in the computational simulations.

The computational simulation results provides quantitative characteristics of the streamlines,

vorticities and topological features of the flow structures. In figure (8) the streamlines are superimposed to the iso-vorticiy surface.

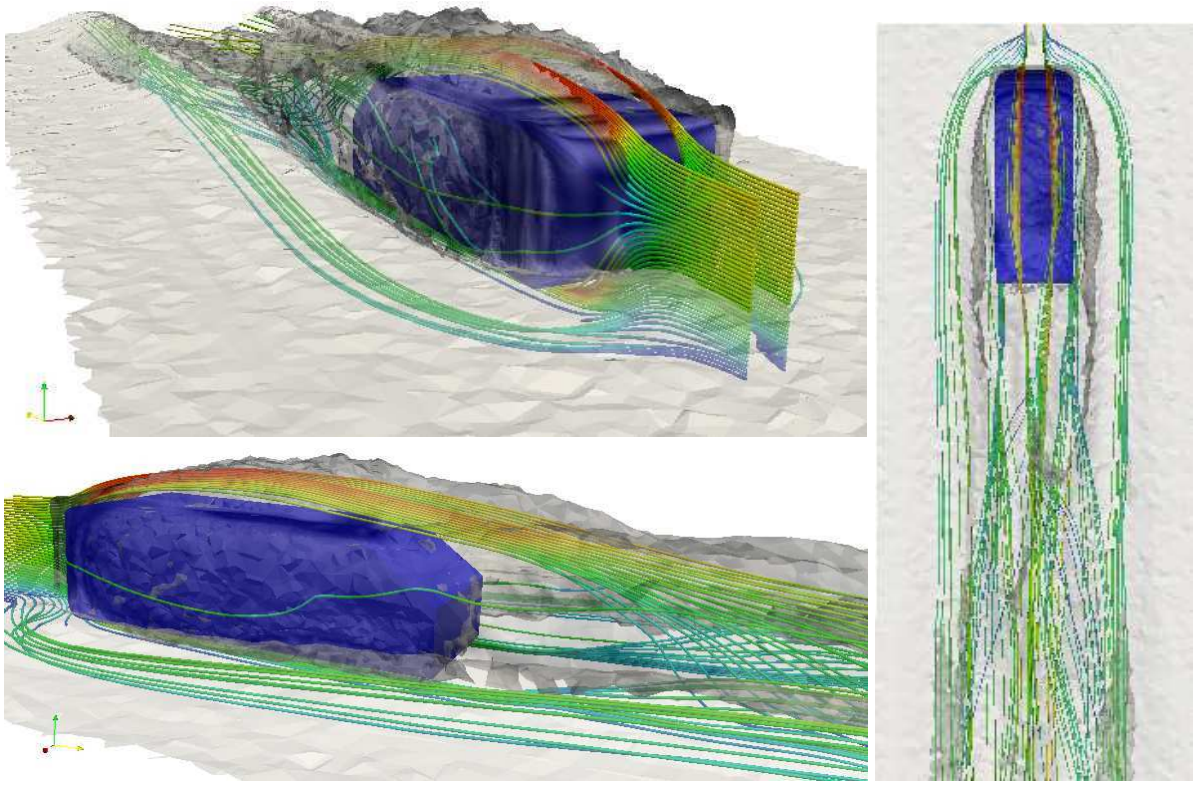

Figure 8: Streamlines and iso-vorticity surface visualization.

4 WIND TUNNEL TESTS

Experimental tests have been performed in the boundary layer wind tunnel facility of the Univesidad Nacional del Nordeste (UNNE). "Jacek Gorecki" wind tunnel has a 2.40 m wide, 1.80 m tall and 22.4 long test section. Details can be found in the work of (Wittwer and Möller, 2000).

A model of scale 1:1 was built with three interchangeable rear ends for slanted angles of 25°, 30° and 35°. The wind tunnel blockage ratio was equal to $0.112/4.32 = 0.025\%$ based on maximum projected frontal area of the model, thus no corrections were made for blockage. All tests were conducted without floor roughness elements, figure (9). Mean velocities were determined from dynamic pressures obtained by means of a Pitot-Prandtl tube connected to a Betz micromanometer.

Time averaged pressure distribution and forces were measured for several angles, namely 25°, 30° and 35°. For the sake of simplicity and comparision with the results obtained from the numerical simulations, only the results associated with the later angle will presented in this work. No visualization techniques (smoke flow, surface oil flow) and flow field measurements were implemented at the moment. These studies remains to be done in a future work.

Figure 9: Ahmed body on the test section of the UNNE wind tunnel.

Another experimental work was used as a reference to compare with the experimental tests. Lienhart and Becker (2003) performed detailed Laser Doppler Anemometry (LDA), hot-wire anemometry and static pressure measurements in a low-speed wind tunnel with a bulk velocity of 40 m/s. This comprehensive study provides valuable information to perform comparisions with numerical and/or experimental data and is used in this work to corroborate both simulations.

4.1 Drag measurements

Time-varying forces were measured using a strain gage balance built especifically for drag measurements tests. It consists of two steel plates suported internally by four steel sheets instrumented with strain gages to measure its deformations, see figure (10). The strain gages are connected into a Wheatstone half bridge and the output voltage is passing through a Vishay System 2100 signal conditioner and then to a Computer Board's PCI-DAS 1602 data acquisition board of 16 channels.

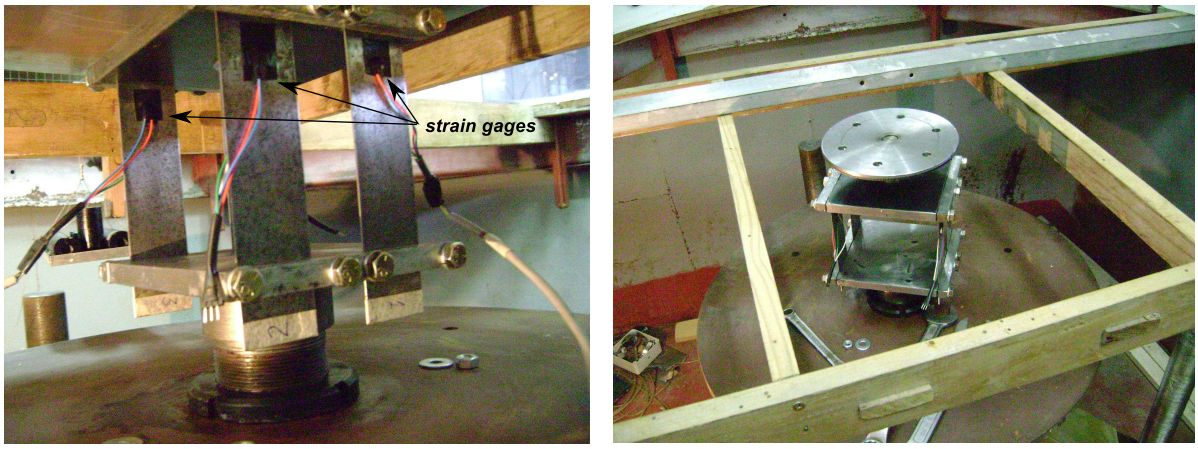

Figure 10: Strain gage balance for drag measurements.

Each record had an extension of 20 seconds, with an acquisition rate of 500 Hz and lowpass filtered with a digital filter at a 12 Hz cut-off frequency, figure (11).

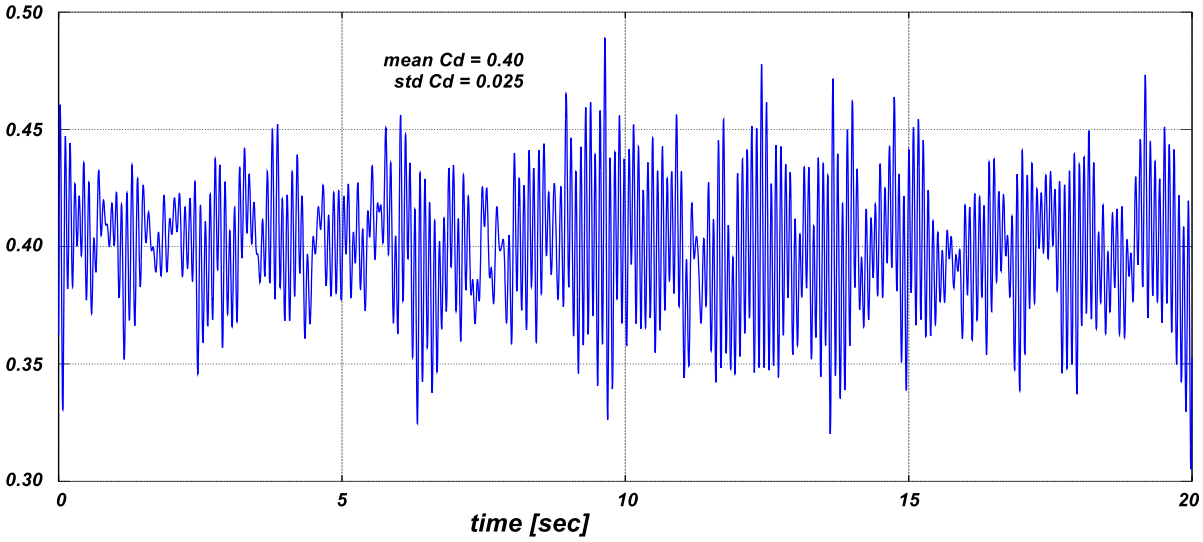

Figure 11: Drag coefficient history.

4.2 Pressure measurements

The pressure was obtained on the rear end of the model through surface pressure measurements using a differential pressure electronic transducer Micro Switch Honeywell 163 PC. A sequential switch Scanivalve 48 D9-1/2 driven by a CTLR2/S2-S6 solenoid controller connected the model pressure taps to the transducer through PVC tubes. A detail can be seen in figure (12). Only one half of the rear slant and vertical surfaces were instrumented.

Figure 12: Detail of the pressure taps in the model.

Pressure coefficients distribution on the rear slanted plane is shown in figure (13) with the experimental results from the work of Lienhart and Becker (2003). Likewise, pressure coefficients distribution on the rear vertical plane is shown in figure (14) and compared with the same experimental reference.

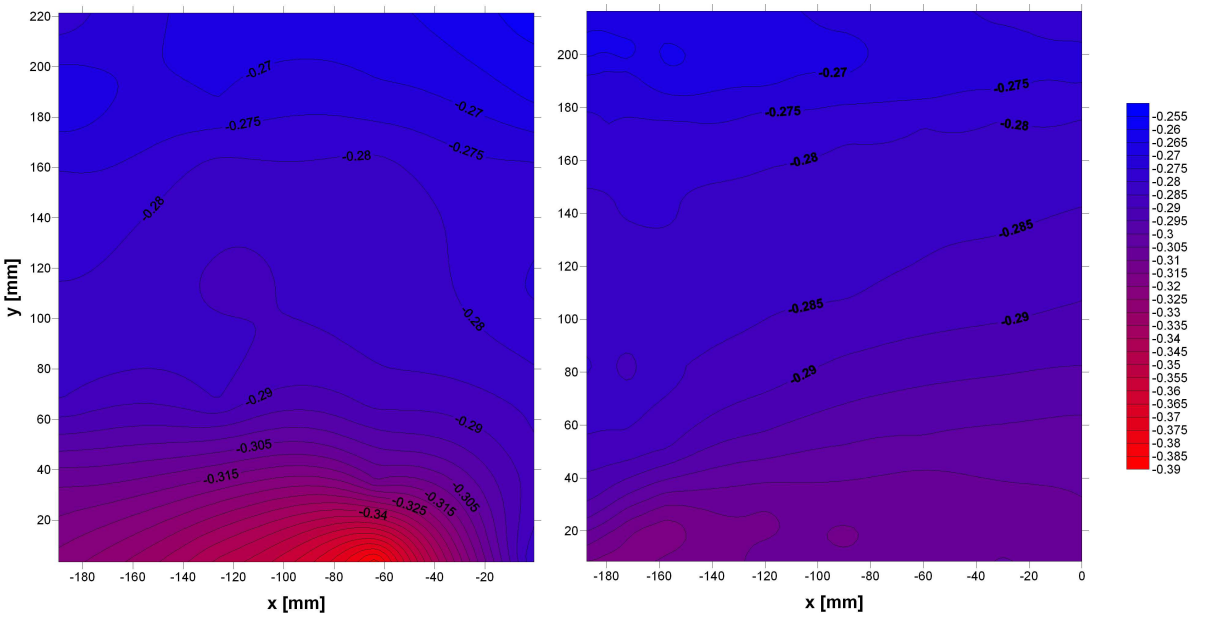

Figure 13: Pressure coefficients distribution over the rear slanted plane of the model: from this work (*left*) and from the experimental work of Lienhart and Becker (2003) (*right*).

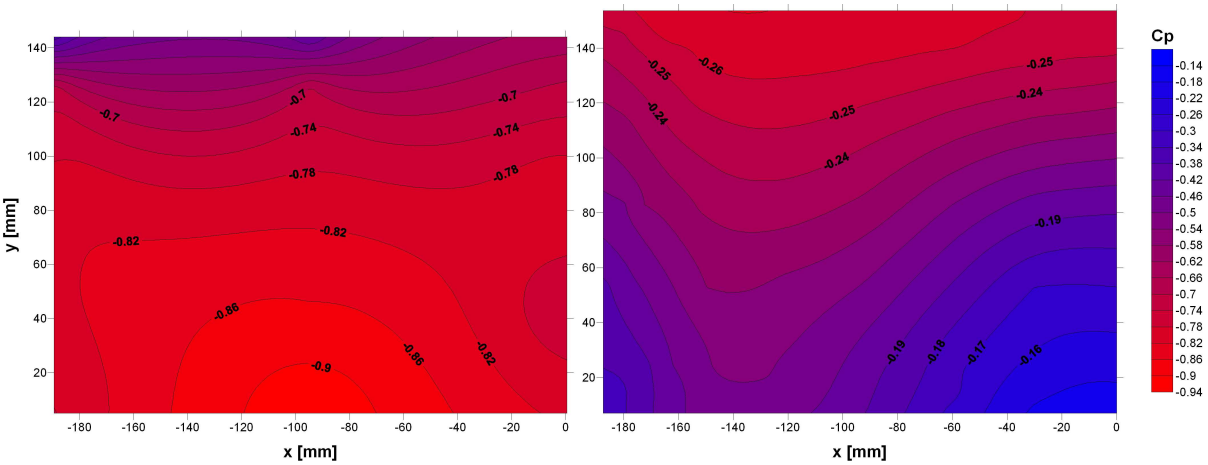

Figure 14: Pressure coefficients distribution over the rear vertical plane of the model: from this work (*left*) and from the experimental work of Lienhart and Becker (2003) (*right*).

5 FURTHER CONSIDERATIONS

Once the numerical and experimental methodologies here discused will be improved and effectively used, the next step is the consideration of the dynamic characteristics of the vehicles which with the addition of the turbulent flow will result and a fluid-structure interaction (FSI) problem.

In the numerical simulation sense, the simultaneous solution of the fluid and structure equations for complex/large scale problems using a "monolithic" scheme may be mathematically unmanageable or its implementation can be a laborious task. An efficient alternative is to solve each subproblem in a partitioned procedure where time and space discretization methods could

be different. Such a scheme simplifies explicit/implicit integration and it is in favor of the use of different codes specialized on each area.

An staggered fluid/structure coupling algorithm is currently implemented in the PETSc-FEM code (Storti et al., 2009) and the analysis of the aeroelastic processes developed during the starting phase of a rocket engine was succesfully accomplished (Garelli et al., 2010).

In the experimental field, the next step is to simulate accurately some vehicle dynamic behaviours like yaw, pitch and roll motion under the external forces of the wind. This tasks will provide data to calibrate the numerical algorithm in PETSc-FEM.

6 CONCLUSIONS

This work presents the first preliminary results of the experimental and numerical determination of pressure coefficients and aerodynamic forces on bluff bodies exposed to a turbulent flow.

Experimental and numerical analysis of the flow over the Ahmed body with a 35° rear slanted angle were performed. Ahmed body was choosen as a standard reference given that it was numerically and experimentally studied in an exhaustive way.

Comparing both, results from the experimental tests made in this work and the other experimental reference as well as the provided by the computational simulation presents some appreciable differences. Mean drag force in the experimental tests ($Cd_{mean} = 0.40$) presents a high value when comparing with the obtained by Ahmed et al. (1984) ($Cd_{mean} = 0.257$) while the numerical obtained value had a difference lower than a 9% ($Cd_{mean} = 0.28$). Is important to note that both values corresponds to the model with the four stilts whereas in the work of Ahmed et al. (1984) the total drag has been corrected for tare drag of stilts. To account for this, a numerical simulation of the model with the stilts was performed. The results from figure (5) ($Cd_{mean} = 0.357$) reflects the importance of this consideration. Nevertheless, experimental values are still higher.

From figures (13) and (14) it can be shown that pressure measured in the wind tunnel on the rear slanted plane are almost in agreement with those of (Lienhart and Becker, 2003) in spite of the low Reynolds number (in our case is of 1.7×10^6) while for the rear base of the model significantly exceeds the reported values. This results explains the differences in the drag forces. In the experimental tests, the flow is accelerated in the lower zone of the rear base possibly due to a mass of air entering into the test section in the drag balance hole by suction. Improvement of the experimental equipment is a work currently in progress.

7 ACKNOWLEDGMENTS

This work has received financial support from *Consejo Nacional de Investigaciones Científicas y Técnicas* (CONICET, Argentina, grant PIP 5271/05), *Agencia Nacional de Promoción Científica y Tecnológica* (ANPCyT, Argentina, grants PICT 01141/2007, PICT 2008-0270 “Jóvenes Investigadores”, PICT-1506/2006), *Universidad Nacional del Litoral* (UNL, Argentina, grants CAI+D 2009 65/334) and *Secretaría de Ciencia y Técnica de la Universidad Tecnológica Nacional, Facultad Regional Resistencia* (Chaco).

REFERENCES

Ahmed S.R., Ramm G., and Faltin G. Some salient features of the times-averaged ground vehicle wake. *Society of Automotive Eng., Inc*, 1:1–31, 1984.

Basara B., Przulj V., and Tibaut P. On the calculation of external aerodynamics industrial benchmarks. *SAE paper*, 2001-01-0701, 2001.

Cooper K. Bluff-body aerodynamics as applied to vehicles. *Journal of Wind Engineering and Industrial Aerodynamics*, 49:1–22, 1993.

Davison L. Hybrid LES-RANS: inlet boundary conditions for flows including recirculation. In *TSFP5 - 5th International Symposium on Turbulence and Shear Flow Phenomena*, volume 2, pages 689–694. Munich, 2007a.

Davison L. Using isotropic synthetic fluctuations as inlet boundary conditions for unsteady simulations. *Advances and Applications in Fluid Mechanics*, 1:1–35, 2007b.

Franck G., Carazo F., Nigro N., Storti M., and J. D. Numerical simulation of the flow around the ahmed vehicle for a critical slant angle. In *Enief 2004, XIV Cong. on Num. Meth.*, pages 2189–2209. Bariloche, Argentina, 2004.

Franck G., Nigro N., Storti M., and J. D. Modelización del flujo del viento en el modelo de ahmed. In *Enief 2003, XIII Cong. on Num. Meth.*, pages 124–142. Bahía Blanca, Argentina, 2003.

Garelli L., Paz R., and Storti M. Fluid-Structure interaction study of the start-up of a rocket engine nozzle. *Computers & Fluids*, 39:1208–1218, 2010.

Guilmineau E. Computational study of flow around a simplified car body. *Journal of Wind Engineering and Industrial Aerodynamics*, 96(6-7):1207 – 1217, 2008. ISSN 0167-6105. doi:DOI:10.1016/j.jweia.2007.06.041. 5th International Colloquium on Bluff Body Aerodynamics and Applications.

Hinterberger C., García-Villalba M., and Rodi W. Large eddy simulation of flow around the ahmed body. *Lectures Notes in Applied and Computational Mechanics, The Aerodynamics of Heavy Vehicles: Trucks, Buses and Trains*, McCallen, F. Browand, J. Ross (Eds.), Springer Verlag, 2004.

Krajnovic S. *Large eddy simulations for computing the flow around vehicles*. Ph.D. thesis, Dept. of Thermo and Fluid Dynamics, Chalmers University of Technology, Gothenburg, 2002.

Krajnovic S. and Davison L. Large eddy simulation of the flow around a simplified car model. In *2004 SAE World Congress*, volume SAE Paper 2004-01-0227. Detroit, Michigan, USA, 2004a.

Krajnovic S. and Davison L. Large Eddy Simulation of the flow around a simplified car model. In *Proceedings of the ASME Heat Transfer/Fluids Engineering Summer Conference 2004*, pages 653–662. 2004b.

Lienhart H. and Becker S. Flow and turbulence structure in the wake of a simplified car model. *SAE paper*, 2003-01-0656, 2003.

Storti M., Nigro N., Paz R., and Dalcín L. Strong coupling strategy for fluid-structure interaction problems in supersonic regime via fixed point iteration. *Journal of Sound and Vibration*, 320:859–877, 2009.

Tabor G. and Baba-Ahmadi M. Inlet conditions for large eddy simulation: A review. *Computers and Fluids*, 39:553–567, 2010.

Wittwer A. and Möller S. Characteristics of the low speed wind tunnel of the UNNE. *Journal of Wind Engineering and Industrial Aerodynamics*, 84:307–320, 2000.